The vimentin cytoskeleton regulates focal contact size and adhesion of endothelial cells subjected to shear stress

Daisuke Tsuruta and Jonathan C. R. Jones*

Department of Cell and Molecular Biology, Northwestern University Medical School, Morton 4-616, 303 E. Chicago Avenue, Chicago, IL 60611, USA

*Author for correspondence (e-mail: j-jones3@northwestern.edu)

Accepted 6 August 2003
Journal of Cell Science 116, 4977-4984 © 2003 The Company of Biologists Ltd
doi:10.1242/jcs.00823

Summary

Recently, we reported that vimentin-type intermediate filaments, in addition to microfilaments, associate with αvβ3 integrin-positive focal contacts in endothelial cells. To gain insight into intermediate filament-focal contact interaction, we induced expression of yellow fluorescent protein (YFP)-integrin β3 and cyan fluorescent protein (CFP)-vimentin protein in endothelial cells. At least 50% of the YFP-β3 integrin-labeled focal contacts associated with CFP-labeled vimentin intermediate filaments in live cells. Moreover, focal contacts and intermediate filaments moved in concert in the plane of the membrane and assembling focal contacts were sites of vimentin filament assembly. When endothelial cells were subjected to flow, large focal contacts assembled and associated with thick vimentin bundles. These large focal contacts showed minimal dynamic activity. Cells in which vimentin expression had been inhibited by RNA interference assembled smaller than normal focal contacts. More dramatically, such cells showed decreased adhesion to the substratum. These data provide evidence that the vimentin cytoskeleton regulates focal contact size and helps stabilize cell-matrix adhesions in endothelial cells.

Movies available online

Key words: Intermediate filament, Integrin, Matrix adhesion

Introduction

The interaction of cells with the extracellular matrix plays a crucial role in development and during periods of tissue remodeling by regulating tissue architecture and function. In many cell types, the molecules involved in cell-matrix adhesion are concentrated in specific morphological entities called focal contacts (FCs) (Hynes, 1992; Hynes, 2002; Simon and Burridge, 1994; Smilenov et al., 1999; Zamir et al., 2000). Within each FC, cell surface receptors of the integrin family cluster together and interact with extracellular matrix ligands on the outside of the cell and with the actin-microfilament system in the cytoplasm (Hynes, 1992; Hynes, 2002; Simon and Burridge, 1994; Smilenov et al., 1999; Zamir et al., 2000). Indeed, FCs or, rather, their components not only function to mediate cell-matrix adhesion but also serve as a surface anchor for the cytoskeleton and as transducers of signals from the matrix to the cell and vice versa (Howe et al., 1998; Hynes, 1992; Hynes, 2002).

Typically, FCs are considered to tether actin-containing microfilaments to the cell surface (Simon and Burridge, 1994). However, recently we provided evidence that the majority of αvβ3 integrin-rich FCs located at the edge of several endothelial cell types show association with both the microfilament and vimentin intermediate filament (IF) cytoskeletons (Gonzales et al., 2001). We termed these vimentin-associated matrix adhesions (VMAs). There is precedent for our observation since, as long ago as 1987, Bershadsky et al. demonstrated that in quail embryo fibroblasts vimentin IFs are connected to FCs (Bershadsky et al., 1987). Moreover, the idea that vimentin IFs are involved in modulating either the structure or function of FCs is also supported by observations of the organization of FCs along regions of cell-matrix interaction in vimentin-deficient fibroblasts (Eckes et al., 1998). Specifically, FCs in vimentin-null cells do not distribute geometrically. Rather their longitudinal axes are randomly orientated. In sharp contrast, FCs distribute in an orderly pattern. Nonetheless, the concept that vimentin IFs associate directly with FCs and may regulate their structure and/or function is not widely accepted. Thus, to provide further support for this idea and to study the functional implication of such associations we have used cell imaging techniques to study the relative organizations of vimentin and integrins in live endothelial cells. To do so, we induced expression of yellow fluorescent protein-tagged integrin β3 subunit (YFP-β3) and cyan fluorescent protein-tagged vimentin IF protein (CFP-vimentin) in the same endothelial cells and monitored the fate of the tagged proteins in the double-transfectants by confocal laser scanning microscopy. Furthermore, we have studied the fate of vimentin IF and β3 integrin subunits in endothelial cells when the cells were subjected to physiological hemodynamic shear stress in the form of flow. Our results indicate that there is enhancement of vimentin IF connection to FC proteins in cells subjected to flow and that such an association appears involved in stabilizing cell-matrix adhesions.

Materials and methods

Cell culture and transient transfections

Immortalized human bone marrow endothelial cells (TrHBMEC) were kindly provided by Babette Weksler (Weill Medical College of Cornell University, Ithaca, NY) and Denise Paulin (Universite Paris VII and Institut Pasteur, Paris, France) (Schweitzer et al., 1997). TrHBMECs were maintained in Dulbecco's modified Eagle's medium with 10% fetal bovine serum, 1% penicillin/streptomycin, 1% L-glutamine and 1× RPMI 1640 vitamins solution (Gonzales et al., 2001; Tsuruta et al., 2002). Cell cultures were kept in a humidified 5% CO_2/95% air incubator at 37°C. In some experiments, cells were treated with 0.1 μM cytochalasin D (Sigma Chemical Co., St. Louis, MO). Prior to transfection, TrHBMECs were trypsinized and resuspended in N-(2-hydroxyethyl) piperazine-2′-(2-ethanesulphonic acid) (Hepes)-buffered DMEM at about 8×10^6 cells/ml. The cells were electroporated with DNA at 950 μFD, 186 ohm, and 210 V in a BTX Electro Cell Manipulator 600 (BTX, San Diego, CA).

Mammalian expression vector preparation

cDNA encoding full-length human β3 integrin and vimentin were prepared as detailed elsewhere (Tsuruta et al., 2002; Yoon et al., 1998). These were then ligated into CFP-N1 or YFP-N1 vectors according to the instructions of the suppliers (Clontech Laboratories Inc., Palo Alto, CA).

Antibodies

The LM609 mouse monoclonal antibody against αvβ3-heterodimer, rabbit anti-β3 integrin sera, mouse monoclonal anti-actin and rat monoclonal anti-tubulin were purchased from Chemicon International, Inc. (Temecula, CA). The mouse monoclonal antibody specific for vimentin (clone V9) was purchased from Sigma Chemical Co. (St. Louis, MO). Mouse monoclonal antibody against GFP (clones 7.1 and 13.1) was purchased from Roche Inc. Rhodamine-conjugated phalloidin was obtained from Molecular Probes (Eugene, OR). Secondary antibodies conjugated to fluorochromes or horseradish peroxidase were purchased from Jackson ImmunoResearch Labs Inc. (West Grove, PA).

Transfection of TrHBMECs with vimentin siRNA

1×10^5 TrHBMECs were seeded onto 40 mm Bioptechs coverslips in 6 ml DMEM containing serum and antibiotics. Cells were incubated for 1 day under 37°C and 5% CO_2. Cells were transfected with vimentin short interference RNA (siRNA) using TransMessenger Transfection Reagent, both purchased from Qiagen Inc. (Valencia, CA), following the company protocol (Harborth et al., 2001; Elbashir et al., 2001). As a control, a non-specific 5′-fluorescein-conjugated siRNA was used (Qiagen).

Immunofluorescence

Endothelial cells, grown on glass coverslips, were fixed in 3.7% formaldehyde in PBS for 5 minutes and extracted in 0.5% Triton X-100 in PBS for 10 minutes at 4°C to allow subsequent antibody penetration. After extensive washing in PBS, the fixed and extracted cells were incubated with primary antibodies at 37°C in a humid chamber for 1 hour, washed three times in PBS, and then incubated with the secondary antibody for an additional 1 hour at 37°C as detailed elsewhere (Tsuruta et al., 2002). Stained specimens were viewed using an LSM510 laser scanning confocal microscope (Gonzales et al., 2001).

Protein preparations, SDS-PAGE and western immunoblotting

Cell populations were solubilized in SDS sample buffer consisting of 8 M urea, 1% SDS in 10 mM Tris-HCl, pH 6.8, and 15% β-mercaptoethanol. Proteins were separated by SDS-PAGE, transferred to nitrocellulose, and processed for immunoblotting as previously described (Laemmli, 1970).

Live cell observation

For live cell studies, cells on coverslips were placed on a Bioptechs chamber (Bioptechs Inc., Butler, PA). The closed chamber preparation was maintained at 37°C in Leibovitz's L-15 medium supplemented with 10% fetal bovine serum, 1% penicillin/streptomycin, 1× RPMI 1640 vitamins solution, 100 μM 6-hydroxy-2,5,7,8-tetramethyl-chroman-2-carboxylic acid (Trolox®; Sigma Chemical Co., St Louis, MO) and 20 μM ascorbic acid (Sigma Chemical Co., St Louis, MO) with an incubator on the stage of either an LSM510 confocal (Zeiss Inc., Thornwood, NY) or a Nikon ECLIPSE TE 2000-U microscope (Nikon Instruments Inc., Melville, NY). CFP images were acquired by excitation at 433 nm and emission at 466 nm, while YFP images were acquired by excitation at 512 nm and emission at 555 nm. Phase-contrast images of cells were taken both before and after time-lapse observations. Images from cells that had undergone gross morphological changes during the period of observation were discarded.

The size of focal contacts was determined by quantifying pixels in matrix adhesions in cells that were stained with antibody against the αvβ3 integrin. This was done using MetaMorph 4.0 software (Universal Imaging). Data were analyzed using Microsoft Excel (Microsoft Corporation, Redmond, WA). Statistical significance was estimated by paired *t*-test. A probability value under 0.05 was considered significant.

Fluid shear stress

To induce shear stress, TrHBMECs maintained in the Bioptechs apparatus on the stage of a microscope were exposed to fluid shear stress generated by perfusing culture medium over the cells. The pH of the system was kept constant by gassing with 5% CO_2/95% air and the temperature was maintained at 37°C. A shear stress of 12 dynes/cm^2 was used in all experiments. This is within the physiological range of shear stress to which endothelial cells are subject in human arteries (DePaola et al., 1999).

Results

Characterization of expression of CFP-vimentin and YFP-β3 integrin in TrHBMECs

We used the endothelial cell line TrHBMEC derived from bone marrow for these studies. These cells have been shown by us and others to display normal endothelial cell properties including the ability to assemble into nascent blood vessels in vitro and expression of endothelial cell basement membrane components, integrins and markers such as CD151 (Gonzales et al., 2001; Gonzalez et al., 2002; Schweitzer et al., 1997). To initiate our studies TrHBMECs were transfected with mammalian expression vectors encoding CFP-vimentin or YFP-β3 integrin. Western blot analyses of protein extracts of the transiently co-transfected TrHBMEC populations using anti-GFP antibodies confirmed expression of proteins of the appropriate molecular mass: 82 kDa for CFP-vimentin and 132 kDa for YFP-β3 integrin (Fig. 1A, lane 1). Furthermore, we evaluated the same extracts using an anti-integrin β3 serum, which reacts with both YFP-tagged and endogenous β3 integrin (Fig. 1A, lane 2). Likewise, an anti-vimentin antibody recognizes CFP-tagged and endogenous vimentin proteins (Fig. 1A, lane 3).

TrHBMECs, transfected with constructs encoding YFP-β3

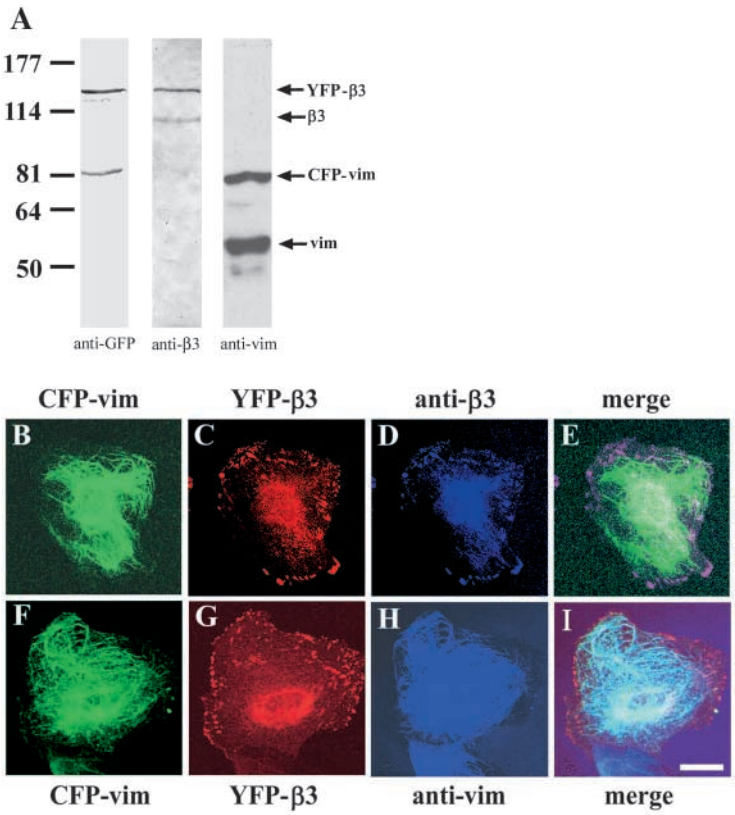

Fig. 1. Characterization of CFP-vimentin and YFP-β3 integrin expression in TrHBMEC transfectants. (A) Extracts of transformed human bone marrow endothelial cells (TrHBMECs) co-transfected with expression vectors encoding CFP-vimentin and YFP-β3 integrin were processed for western immunoblot analysis using antibodies against GFP (lane 1), β3 integrin (lane 2) or vimentin (lane 3). Molecular masses are indicated on the left. The reactive species are indicated on the right. (C-I) Images of transfected TrHBMECs. Cells expressing CFP-vimentin (B,F) and YFP-β3 integrin (C,G) were fixed and then processed for immunofluorescence microscopy using an anti-β3 integrin subunit antiserum (D) or anti-vimentin antibodies (H). E and I are the merged images of B-D and F-H, respectively. YFP-β3 integrin (C) colocalizes precisely with the endogenous αvβ3 integrin complexes in FC (D) (purple in the merged image in E). CFP-vimentin (B) colocalizes precisely with the endogenous vimentin intermediate filaments (H) (sky blue in the merged image in I). Scale bar: 10 μm. Vim, vimentin.

integrin and CFP-vimentin were viewed by confocal immunofluorescence microscopy using antibodies recognizing either β3 integrin or vimentin to ensure that the protein products of the transgenes behave normally in the double transfectants (Fig. 1B-E and F-I respectively). In the dual transfected cells, staining generated by YFP-β3 integrin proteins mirrored exactly the staining produced by β3 integrin antibodies at the site of FCs (Fig. 1C,G). Likewise, CFP-vimentin protein precisely incorporated into filament arrays stained by the vimentin antibodies (Fig. 1F,I). In both sets of images vimentin IFs associated with a subset of FCs that were located towards the cell periphery.

Dynamics of vimentin and integrin β3 subunit in live TrHBMECs

We next analyzed the fate of CFP-vimentin and YFP-β3 integrin in double transfectants within populations of live TrHBMEC cultures for periods of up to 60 minutes. Consistent with our previous observations, β3 integrin-positive FCs showed movement within the plane of the membrane (Tsuruta et al., 2002) (Fig. 2). Moreover, in more than twenty cells analyzed in this way, at least 50% of FCs showed some association with the vimentin cytoskeleton (Gonzales et al., 2001). More intriguingly, we have observed various ‘behaviors’ of vimentin IFs in the dual transfectants (Fig. 2; see also movies

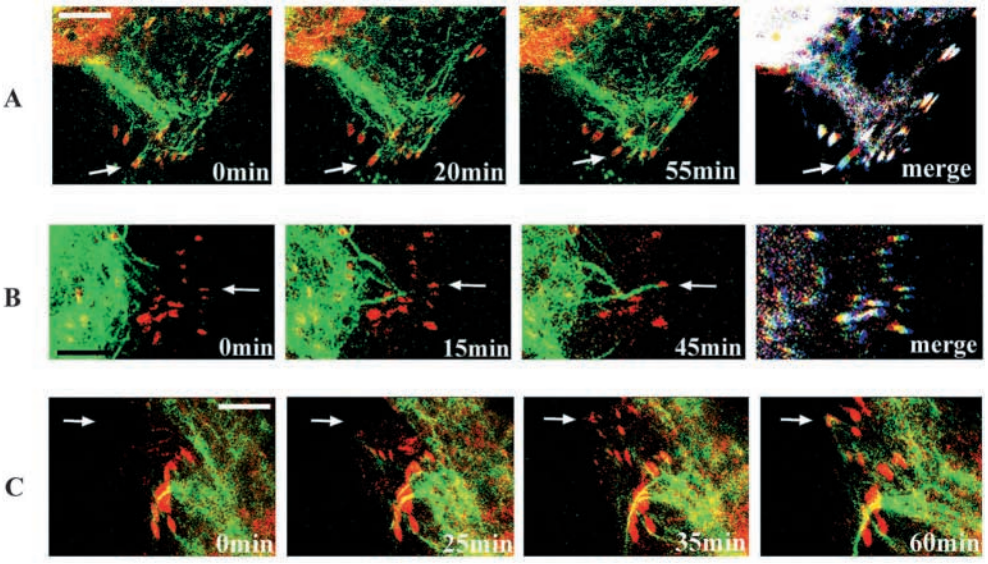

Fig. 2. The dynamics of vimentin IFs and β3 integrin-rich FCs in TrHBMEC transfectants. TrHBMECs co-expressing YFP-β3 integrin and CFP-vimentin were followed over periods up to 60 minutes in the live state. A-C reflect different types of interactions and relative behaviors of vimentin IFs and FCs in double transfectants. (A,B) The signals for the three time points were coded blue, green and red, with the final panel reflecting all three images merged. In A, a YFP-β3 integrin-containing FC moves centripetally in concert with vimentin IF (arrow). (B) Vimentin IFs elongate from the perinuclear zone towards an FC (arrow) at the edge of the cell. (C) A newly assembled FC (arrow) appears and establishes contact with vimentin IF. Scale bar: (A) 5 μm, (B,C) 3 μm. A, B and C can be viewed in video form (movies 1, 2 and 3, http://jcs.biologists.org/supplemental/).

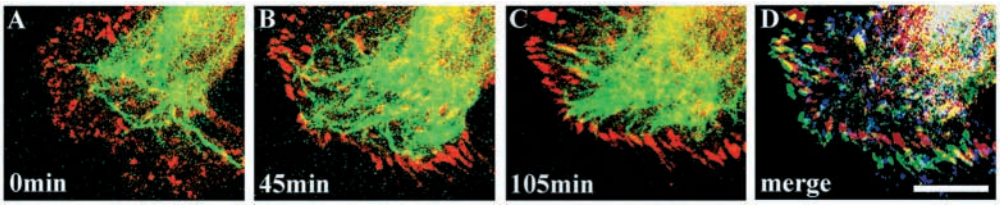

Fig. 3. The dynamics of vimentin IF and β3 integrin-rich FCs following initiation of flow and during the subsequent 105 minutes. (A) TrHBMEC co-expressing YFP-β3 integrin and CFP-vimentin were followed over a period of 105 minutes in the live state after the exposure to flowing medium at 12 dynes/cm^2. The YFP images at 0, 45 and 105 minutes were coded in blue, green and red, respectively, and then overlaid. Note that FCs are dynamic during the viewing period as revealed by the rainbow color effect in D. Scale bar: 5 μm. This can be viewed in video form (movie 4, http://jcs.biologists.org/supplemental/).

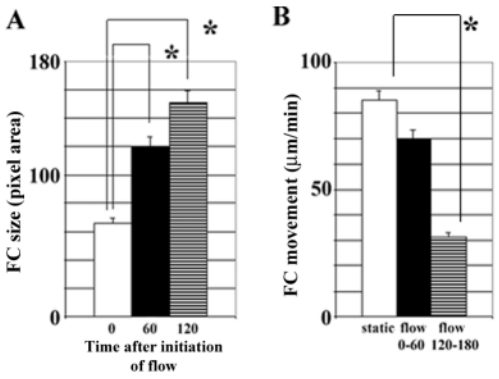

Fig. 4. Quantification of FC size and motility under static and flow conditions. (A) The size of FCs in cells was quantified by counting pixels of labeled FCs at 0, 60 and 120 minutes after the initiation of shear stress, in the form of flowing medium at 12 dynes/cm^2. (B) Movement of FCs was assayed in non-treated (static) cells and in cells subjected to flow over periods 0-60 and 60-120 minutes after the initiation of shear stress. A total of 40 FCs in three cells were evaluated for each time point. *Indicates a significant difference (P<0.01).

1, 2 and 3, http://jcs.biologists.org/supplemental/). In some cells, vimentin filaments appeared to move in concert with FCs centripetally (Fig. 2A; see also movie 1, http://jcs.biologists.org/supplemental/). In Fig. 2B, the area of the cell shown contains FCs that exhibit little association with vimentin. However, during the period of analysis, vimentin filaments extend from the perinuclear zone and subsequently make contact with FCs positioned towards the cell edge (Fig. 2B; see also movie 2, http://jcs.biologists.org/supplemental/). In yet other cells, newly assembled FCs, which some investigators term focal complexes, appeared to be the site of vimentin filament nucleation or assembly (Fig. 2C; see also movie 3, http://jcs.biologists.org/supplemental/) (Zamir et al., 2000).

The dynamics of vimentin filament and β3 integrin-rich focal contacts under flow

In vivo endothelial cells are subjected to mechanical stress in the form of blood flowing over their surfaces (Davies et al., 1997; Davies et al., 1994; Galbraith et al., 1998). To assess what impact such flow may have on the structure and dynamics of FCs and the vimentin IF cytoskeleton, TrHBMECs co-expressing CFP-vimentin and YFP-β3 integrin were placed under flow conditions at a force of 12 dynes/cm^2. During the first 100-120 minutes after the initiation of flow, FCs in TrHBMECs underwent a dramatic and significant increase in size, consistent with other reports (Galbraith et al., 1998) (Fig. 3, Fig. 4A; see also movie 4, http://jcs.biologists.org/supplemental/). However, they also showed an increase in their interaction with vimentin IF. A typical example of this dramatic phenomenon is provided in Fig. 3 (movie 4, http://jcs.biologists.org/supplemental/). As the FCs enlarge they show centripetal movement (Fig. 3D). We calculated the mean displacement of FCs over the period 0-60 minutes after the initiation of flow in over 40 endothelial cells (Fig. 4B). Although the value is somewhat smaller than that observed for FCs in untreated cells, the difference was not significant (Fig. 4B). Nonetheless, this indicates that flow may induce a gradual slowing in FC movement. To assess this possibility we next followed the fate of the large FCs and their associated vimentin bundles in live cells for the period 120-220 minutes during flow treatment (Fig. 5; see also movie 5, http://jcs.biologists.org/supplemental/). Images of a typical transfected live TrHBMEC at 120, 170 and 220 minutes during flow are provided in Fig. 5. FCs in this cell were stable throughout the 100 minutes of observation (Fig. 5D). We have quantified the displacement of FCs in more than 40 cells over the period 120-180 minutes during flow treatment. The results are presented in Fig. 4B and reveal that FCs in cells subjected to prolonged flow show dramatically less dynamic properties.

In addition to analyzing the movement and size of FCs in TrHBMEC subjected to flow we also assessed the numbers of assembling and disassembling FCs in untreated cells and cells under flow conditions. The results of our analyses are presented in Table 1. The percentage of stable FCs was significantly increased 120 minutes after the start of flow.

Table 1. Dynamics of focal contacts in TrHBMECs expressing YFP-β3 integrin

	Assembling FCs (%)	Disassembling FCs (%)	Stable FCs (%)
Static (0-60 min) control	20.5±4.6	24.9±5.4*	54.6±8.8†
Static (0-60 min) siRNA	26.1±4.5	33.6±7.6*	40.2±7.4†
Flow (0-60 min)	10.2±1.5	37.4±5.1*	52.5±4.6†
Flow (120-180 min)	12.6±1.5	3.9±1.3*	83.5±1.6†

Static, untreated cells; flow, cells subjected to flow at 12 dynes/cm^2.
Untreated cells were transfected with either control siRNA or vimentin siRNA as indicated.
* and †significant difference (P<0.05).

The dynamics of integrin β3 subunit in vimentin knockdown TrHBMECs

In order to better characterize the potential impact of the

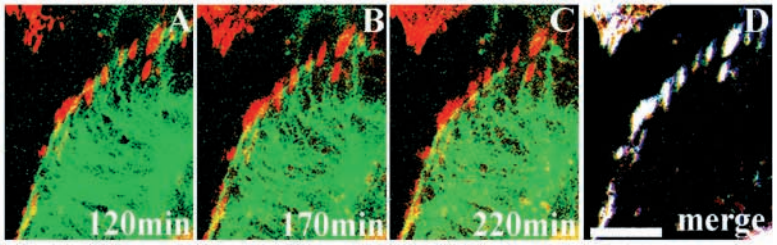

Fig. 5. The dynamics of vimentin filament and β3 integrin-rich focal contacts 120-220 minutes after the initiation of flow. Populations of TrHBMECs co-expressing YFP-β3 integrin and CFP-vimentin was subjected to flowing medium at 12 dynes/cm^2 and then the live cells were viewed for 120-220 minutes after the initiation of shear stress. Images of a typical treated cell at 120, 170, and 220 minutes are shown. The YFP images at (A) 120, (B) 170 and (C) 220 minutes were coded in blue, green and red, respectively and then merged (D). The white colors of the large FCs in D indicate that they show minimal movement in the plane of the membrane. Note also that each FC in A-C shows extensive interaction with vimentin IF. Scale bar: 3 μm. This can be viewed in video form (movie 5, http://jcs.biologists.org/supplemental/).

vimentin cytoskeleton on FC structure and function, we induced a knockdown of vimentin expression using RNA interference (siRNA) technology. We did not use vimentin-null cells derived from the vimentin knockout mouse for these studies because previous work has shown that these cells have abnormalities in their microfilament and microtubule networks (Goldman et al., 1996). Hence, any changes in FCs in these cells may result from the reorganization of the latter networks rather than the lack of vimentin IFs.

At 72 hours following transfection of TrHBMECs with vimentin-specific siRNA, immunoblotting revealed about a 60% reduction in detectable vimentin protein in extracts of the treated endothelial cells (Fig. 6A,B). Moreover, when comparable populations of cells were double stained with antibodies against vimentin in combination with anti-β3 integrin subunit, anti-tubulin antibodies, or rhodamine phalloidin, the majority of cells showed either a complete absence of, or a disrupted vimentin IF network (compare the images in Fig. 6C,E,G with 6D,F,H). The latter was mostly restricted to the perinuclear area (Fig. 6C-H). In contrast, the organization of both the microtubule and microfilament networks appeared unaffected in the same cells (compare Fig. 6F,H with 6E,G). This contrasts with what was observed in the vimentin-null cells mentioned above (Goldman et al., 1996).

We have quantified the effects of the vimentin siRNA treatment in TrHBMECs at 72 hours post-transfection. In 13% of vimentin siRNA-treated TrHBMECs, the vimentin IF network was undetectable while 57% of the TrHBMECs showed a high degree of vimentin IF network disruption. The

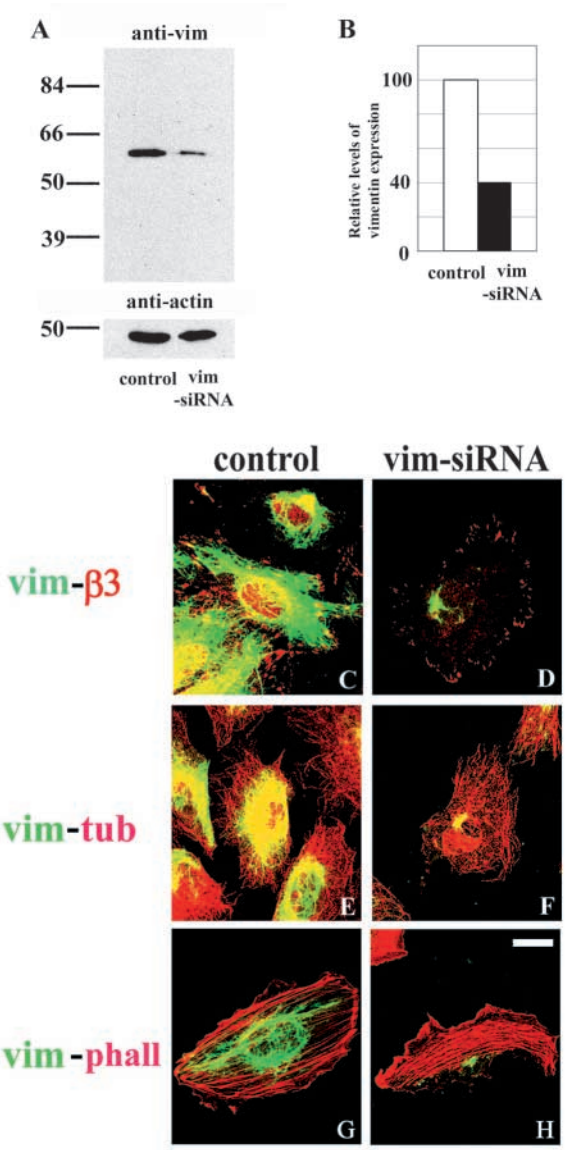

Fig. 6. (A) Western blot of cells transfected with control or vimentin siRNA showing silencing of vimentin in TrHBMECs**.** Extracts of TrHBMECs transfected with control (lane 1) or vimentin siRNA (lane 2) were processed for immunoblot analyses using antibodies against vimentin (upper panel). The blot was re-probed with actin antibody as a loading control (lower panel). Molecular masses are indicated on the left. (B) The immunoblots in A were scanned and analyzed using MetaMorph software. The amount of vimentin in each sample was then normalized to the actin control. Vimentin expression in the control siRNA-treated cells is represented as 100% (white bar). Vimentin expression in the vimentin siRNA-treated cells is reduced by about 60% (black bar). (C-H) Immunofluorescence analyses of cytoskeletal networks and β3 integrin subunits in vimentin siRNA treated TrHBMECs. TrHBMECs were transfected with control siRNA or vimentin siRNA and then 72 hours later were prepared for double label immunofluorescence confocal microscopy using the combinations of antibody or cytoskeleton probes as indicated at the left. The merged images of the two staining patterns are shown in each case. Note that there is a dramatic perturbation in the vimentin cytoskeleton in D, F and H. The FCs labeled by the β3 integrin antibody probe are considerably smaller in D than those labeled by the same probe in C (also see Fig. 9). The vimentin siRNA treatment has minimal, if any, impact on the organization of the microtubule or microfilament networks (compare F and H with E and G). Scale bar: 5 μm.

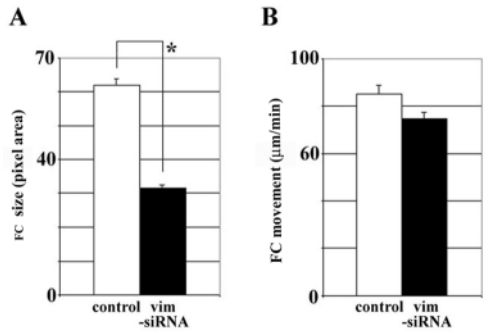

Fig. 7. Quantification of the size and dynamics of FCs in control siRNA and vimentin siRNA-treated TrHBMECs. TrHBMECs were transfected with control siRNA or vimentin siRNA and 72 hours later the size (A) and movement (B) of FCs in the treated cells was evaluated. In all 40 FCs in 3 cells were analyzed in each case. *Indicates a significant difference (P<0.01).

remaining 30% of the treated TrHBMEC population showed a normal pattern of vimentin staining.

Most dramatically, in the vimentin siRNA-treated TrHBMECs, αvβ3 integrin-rich FCs were considerably smaller than FCs in control siRNA-transfected TrHBMECs (compare images in Fig. 6C and 6D). We quantified this effect by counting pixels of labeled FCs under the various treatment regimens and these analyses confirmed our immunofluorescence observations (Fig. 7A). Moreover, the size difference in FCs induced by the vimentin siRNA was also observed in live TrHBMECs that expressed CFP-β3 integrin (compare Fig. 8A and 8B). The impact of vimentin knockdown described here is consistent with studies on fibroblasts derived from the vimentin knockout mouse (Eckes et al., 1998). The FCs in such cells showed an aberrant organization and have been termed ‘irregular’ (Eckes et al., 1998).

We have also monitored the fate of labeled FCs in the vimentin knockdown cells over periods of up to 60 minutes. Movement of FCs in the plane of the membrane of these cells is comparable to control cells (Fig. 7B). Likewise the apparent numbers of assembling and disassembling FCs are not significantly different in control and vimentin siRNA-treated TrHBMECs (Table 1).

We next evaluated the vimentin knockdown cells under flow conditions. Remarkably, when these cells were subjected to flow at 12 dynes/cm^2, within 5-50 minutes the majority of the cells were lost from the substratum (Fig. 9). Indeed, 67% of cells treated with vimentin siRNA (approximately the same percentage of cells that showed disrupted vimentin staining) are unable to maintain substratum adhesion while more than 90% of control siRNA-treated cells remain adherent under the same conditions (Fig. 9G).

We next treated TrHBMECs with cytochalasin D, a known disrupter of microfilaments to assess whether microfilaments play a role in stabilizing FC attachment to the substratum. As we reported previously, the size of FCs in cytochalasin D-treated cells is smaller than in non-treated cells and drug-treated cells undergo arborization (Tsuruta et al., 2002) (Fig. 8C, Fig. 10). After exposing cells to flow, the number of cytochalasin-D-treated cells (Fig. 9E,F) remaining on the substratum was comparable to control siRNA-transfected cells (Fig. 9A,B). Consistent with this resistance to shear stress, the size of FCs in cytochalasin-D-treated cells was significantly larger in cells subjected to flow compared with those cells under static conditions (Fig. 10).

Discussion

FCs were first identified by their appearance in the interference reflection microscope (Abercrombie and Dunn, 1975). They are defined as sites of close contact between cells and the extracellular matrix. The molecular architecture of FCs in a variety of cell types is well defined and their ability to associate with a number of signaling pathways has been established (Hynes, 2002). FCs act as an attachment plaque on the cell surface for the cytoskeleton and, classically, they are considered to show exclusive association with actin-rich microfilaments (Howe et al., 1998; Hynes, 1992; Simon and Burridge, 1994). FCs have also been shown to be sites of microtubule polymerization and microtubules may modulate FC development (Kaverina et al., 2000; Kaverina et al., 1998).

Compared with the large number of studies focused on the role of microfilaments and microtubules in regulating FC structure and/or function, there are few reports that the third major cytoskeleton system, namely the intermediate filament system, even interacts with FCs let alone regulates any of their properties. Yet, a number of studies have indicated that in certain cells FCs show interaction with the vimentin cytoskeleton (Bershadsky et al., 1987; Gonzales et al., 2001). We have extended these observations. In our live endothelial cell populations, we have identified a number of ways in which vimentin IF associate with assembled or newly developed FCs. More importantly, we have analyzed FCs in cells where vimentin expression is knocked down. Remarkably, in such cells FCs are significantly smaller than those observed in untreated cells. It should be noted that the microtubule networks in the vimentin siRNA-treated cells appear normal and therefore it is unlikely that the observed effect of vimentin knockdown on FC size is due to a secondary impact on the microtubule cytoskeleton. Moreover, the size of FCs in cells lacking an intact vimentin cytoskeleton is comparable to that of FCs in cell treated with the microfilament network disrupting drug cytochalasin D. Hence, although

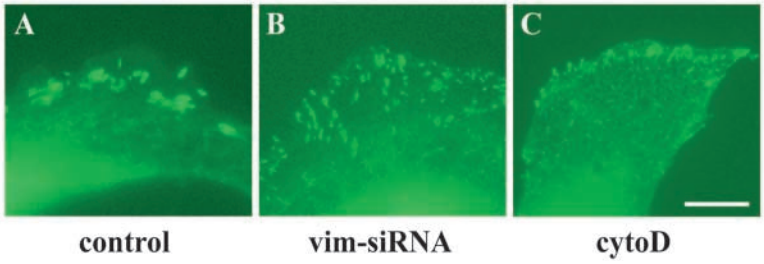

Fig. 8. TrHBMECs treated with vimentin siRNA or cytochalasin D assemble small FCs. TrHBMECs, expressing YFP-β3 integrin, were transfected with control siRNA (A) or vimentin siRNA (B) and after 72 hours were viewed in the live state. In C, TrHBMECs were treated with the 0.1 μM cytochalasin D for 30 minutes prior to observation. Note that FCs appear smaller in B and C than in A. Scale bar: 5 μm.

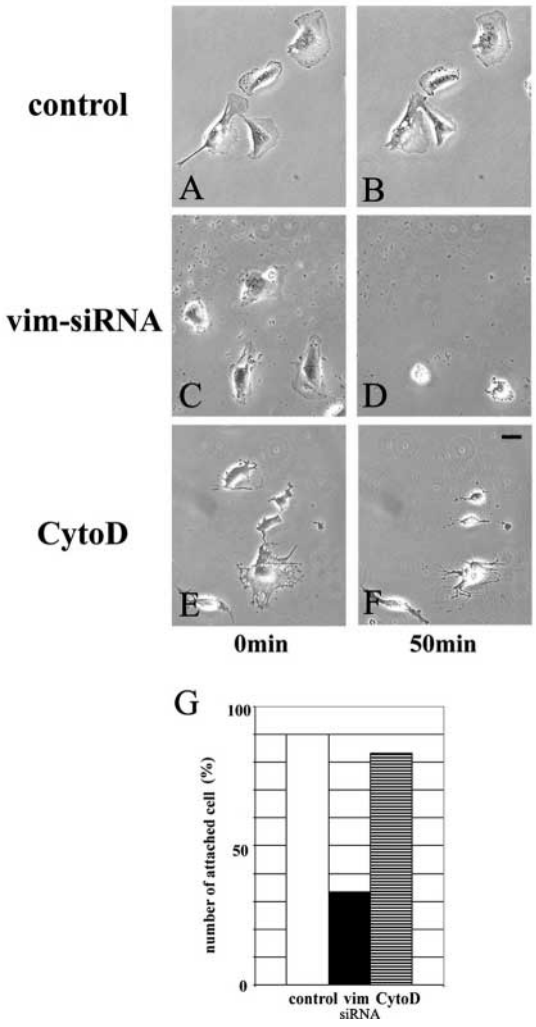

Fig. 9. TrHBMECs treated with vimentin siRNA show reduced adhesion under flow conditions, while those treated with cytochalasin D do not. TrHBMECs were transfected with control siRNA (A,B) or vimentin siRNA (C,D) as indicated and after 72 hours the cells were subjected to flow stress. (E,F) Non-transfected cells were incubated with 0.1 μM cytochalasin D for 30 minutes prior to and during flow treatment. Medium was passed over the cells at 12 dynes/cm^2 as before. Phase contrast images of the cells are shown at 0 and 50 minutes. Scale bar: (in F) 10 μm. (G) The number of cells attached after flow treatment for 50 minutes. Cells were treated with control siRNA, vimentin siRNA or 0.1 μM cytochalasin D (as above). The data were derived from observations of three separate trials involving at least 20 cells per trial.

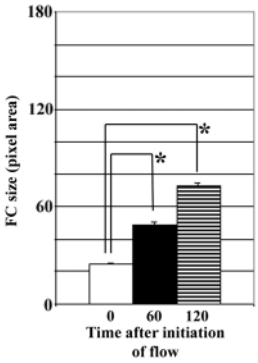

Fig. 10. Quantification of the size of FCs in 0.1 μM cytochalasin D treated TrHBMECs subjected to flow treatment. TrHBMECs were treated with 0.1 μM cytochalasin D for 30 minutes and were then exposed to flow stress for 120 minutes in the presence of the same amount of drug. The size of FCs was evaluated at the indicated time points. In all, 40 FCs in three cells were assayed at each time point. *Indicates a significant difference (P<0.01). Note that FCs show significant enlargement during flow treatment despite the presence of cytochalasin D.

microfilaments appear to play a role in determining the size of FCs, our data provides the first evidence that vimentin also regulates the structure of the FC. This idea is supported by our studies of endothelial cells subjected to mechanical stimulation in the form of flow. Under flow conditions, FCs become large and their motility within the plane of the membrane is considerably slowed or even stopped. This change in movement is correlated with an enhancement in vimentin IF-FC interaction.

How does vimentin regulate FC size? One possibility is that vimentin is involved in the aggregation of ‘clusters’ of FCs in cells. Alternatively, vimentin IF may act as a scaffold holding the FC together. It may well do so by interacting with FC components such as the cytolinker plectin, which we have shown is enriched in the FCs of endothelial cells. In this regard, the idea that vimentin IF stabilizes FC structure and, hence, restricts FC dynamics, is comparable to the way keratin IF stabilize matrix adhesions termed hemidesmosomes (Jones et al., 1998). Specifically, hemidesmosomes lacking IF connections are small or hypoplastic (Gache et al., 1996; Guo et al., 1995).

In addition to a size change, endothelial cells in which vimentin expression has been knocked down show decreased resistance to the effects of flow. A substantial number of the vimentin siRNA-treated cells are removed from their substratum at flow rates of just 12 dynes/cm^2. Hence, since there is no apparent secondary effect of vimentin knockdown on the microtubule or microfilament networks in the siRNA-treated cells, this implies that the vimentin cytoskeleton directly regulates adhesion via an impact on FCs. This supports certain speculations by Eckes and coworkers (Eckes et al., 2000). They reported that in vimentin-knockout animals there is retardation in migration of fibroblasts following wounding. Based on this result, Eckes et al., proposed that disruption of the vimentin IF cytoskeleton may interfere with the ability of fibroblasts to adhere to or tug on matrix molecules (Eckes et al., 2000). Our data provide direct support for this possibility. Moreover, the idea that IFs regulate cell adhesion has a well-established precedent. Keratin IFs stabilize hemidesmosome adhesion to the basement membrane zone (Gache et al., 1996; Guo et al., 1995; Jones et al., 1998).

Endothelial cells in vivo are constantly exposed to hemodynamic forces resulting from the flow of blood. Indeed, fluid shear stress caused by blood flow is a major determinant of remodeling of arteries, the regulation of arterial tone and atherosclerosis (Davies et al., 1997). It has already been established that flow induces an enhanced adhesion of endothelial cells to matrix via their FCs (Davies et al., 1994). Our data imply that vimentin plays an important role in regulating not only FC structure but also function. This raises the issue of why there is no report of blood vessel abnormalities in mice lacking expression of vimentin (Colucci-Guyon et al., 1994). One explanation for this is that there is compensation in the endothelial cells of the vimentin-null mice so that FCs assemble, cluster and adhere to matrix even in the absence of an IF cytoskeleton. Other, non-IF, cytoskeleton components

may compensate for IF loss. Alternatively, blood vessel abnormalities may be manifest only when the null animals are placed under stress or following tissue trauma and/or development of disease. This is supported by the recent finding that wound healing is significantly retarded in the vimentin-null mouse (Eckes et al., 2000).

In conclusion, our results provide the first evidence that IF regulate both the structure and function of FCs. Our data open up a new field of study since a number of important questions remain. What are the molecular links between the vimentin cytoskeleton and integrins at the cell surface? Does plectin mediate vimentin-FC interaction in the same way it attaches keratin IF to hemidesmosomes (Borradori and Sonnenberg, 1999; Jones et al., 1998)? What, if any, role does the vimentin cytoskeleton play in regulating the signaling capabilities of FCs (Hynes, 2002)?

We thank the NIH for grant support (HL067016) to J.C.R.J. Dr Teng-Leong Chew provided valuable assistance that allowed us to complete our live cell imaging analyses.

References

Abercrombie, M. and Dunn, G. A. (1975). Adhesions of fibroblasts to substratum during contact inhibition observed by interference reflection microscopy. *Exp. Cell Res.* **92**, 57-62.

Bershadsky, A. D., Tint, I. S. and Svitkina, T. M. (1987). Association of intermediate filaments with vinculin-containing adhesion plaques of fibroblasts. *Cell Motil. Cytoskel.* **8**, 274-283.

Borradori, L. and Sonnenberg, A. (1999). Structure and function of hemidesmosomes: more than simple adhesion complexes. *J. Invest. Derm.* **112**, 411-418.

Colucci-Guyon, E., Portier, M. M., Dunia, I., Paulin, D., Pournin, S. and Babinet, C. (1994). Mice lacking vimentin develop and reproduce without an obvious phenotype. *Cell* **79**, 679-694.

Davies, P. F., Barbee, K. A., Volin, M. V., Robotewskyj, A., Chen, J., Joseph, L., Griem, M. L., Wernick, M. N., Jacobs, E., Polacek, D. C. et al. (1997). Spatial relationships in early signaling events of flow-mediated endothelial mechanotransduction. *Ann. Rev. Physiol.* **59**. 527-549.

Davies, P. F., Robotewskyj, A. and Griem, M. L. (1994). Quantitative studies of endothelial cell adhesion. *J. Clin. Invest.* **93**, 2031-2038.

DePaola, N., Davies, P. F., Pritchard, W. F., Florez, L., Harbeck, N. and Polacek, D. C. (1999). Spatial and temporal regulation of gap junction connexin43 in vascular endothelial cells exposed to controlled distrubed flows in vitro. *Proc. Natl. Acad. Sci. USA* **16**, 3154-3159

Eckes, B., Colucci-Guyon, E., Smola, H., Nodder, S., Babinet, C., Kreig, T. and Martin, P. (2000). Impaired wound healing in embryonic and adult mice lacking vimentin. *J. Cell Sci.* **113**, 2455-2462.

Eckes, B., Dogic, D., Colucci-Guyon, E., Wang, N., Maniotis, A., Ingber, D., Merckling, A., Langa, F., Aumailley, M., Delouvee, A. et al. (1998). Impaired mechanical stability, migration and contractile capacity in vimentin-deficient fibroblasts. *J. Cell Sci.* **111**, 1897-1907.

Elbashir, S. M., Harborth, J., Lendeckel, W., Yalcin, A., Weber, K. and Tuschl, T. (2001). Duplexes of 21-nucleotide RNAs mediate RNA interference in mammalian cell culture. *Nature* **411**, 494-498.

Gache, Y., Chavanas, S. P. L. J., Wiche, G., Owaribe, K., Meneguzzi, G. and Ortonne, J. P. (1996). Defective expresion of plectin/HD1 in epidermolysis bullosa simplex with muscular dystrophy. *J. Clin. Invest.* **97**, 2289-2298.

Galbraith, C. G., Skalak, R. and Chien, S. (1998). Shear stress induces spatial reorganization of the endothelial cell cytoskeleton. *Cell Motil. Cytoskel.* **40**, 317-330.

Goldman, R. D., Khuon, S., Chou, Y. H., Opal, P. and Steinert, P. M. (1996). The function of intermediate filaments in cell shape and cytoskeletal integrity. *J. Cell Biol.* **134**, 971-983.

Gonzales, M., Weksler, B., Tsuruta, D., Goldman, R. D., Yoon, K. J., Hopkinson, S. B., Flitney, F. W. and Jones, J. C. R. (2001). Structure and function of a vimentin-associated matrix adhesion in endothelial cells. *Mol. Biol. Cell* **12**, 85-100.

Gonzalez, A. M., Gonzales, M., Herron, G. S., Nagavarapu, U., Hopkinson, S. B., Tsuruta, D. and Jones, J. C. R. (2002). Complex interactions between the laminin alpha4 subunit and integrins regulate endothelial cell behavior in vitro and angiogenesis in vivo. *Proc. Natl. Acad. Sci. USA* **99**, 16075-16080.

Guo, L., Degenstein, L., Dowling, J., Yu, Q. C., Wollmann, R., Perman, B. and Fuchs, E. (1995). Gene targeting of BPAG1: abnormalities in mechanical strength and cell migration in stratified epithelia and neurologic degeneration. *Cell* **81**, 233-243.

Harborth, J., Elbashir, S. M., Bechert, K., Tuschl, T. and Weber, K. (2001). Identification of essential genes in cultured mammalian cells using small interfering RNAs. *J. Cell Sci.* **114**, 4557-4565.

Howe, A., Aplin, A. E., Alahari, S. K. and Juliano, R. L. (1998). Integrin signaling and cell growth. *Curr. Opin. Cell Biol.* **10**, 220-231.

Hynes, R. O. (1992). Integrins: Versatility, modulation, and signaling in cell adhesion. *Cell* **69**, 11-25.

Hynes, R. O. (2002). Integrins: bidirectional, allosteric signaling machines. *Cell* **110**, 673-687.

Jones, J. C. R., Hopkinson, S. B. and Goldfinger, L. E. (1998). Structure and assembly of hemidesmosomes. *BioEssays* **20**, 488-494.

Kaverina, I., Rottner, K. and Small, V. J. (1998). Targeting, capture, and stabilization of microtubules at early focal adhesions. *J. Cell Biol.* **142**, 181-190.

Kaverina, I., Krylyshkina, O., Gimona, M., Beningo, K., Wang, Y.-L. and Small, V. J. (2000). Enforced polarisation and locomotion of fibroblasts lacking microtubules. *Curr. Biol.* **10**, 739-742.

Laemmli, U. K. (1970). Cleavage of structural proteins during assembly of the head of bacteriophage T4. *Nature* **277**, 680-685.

Schweitzer, K. M., Vicart, P., Delouis, C., Paulin, D., Draeger, A. M., Langenhuijsen, M. M. A. C. and Weksler, B. B. (1997). Characterization of a newly established human bone marrow endothelial cell line: distinct adhesive prpperties for hematopoitic progenitors compared with human umbilical vein endothelial cells. *Lab. Invest.* **76**, 25-36.

Simon, K. O. and Burridge, K. (1994). Interactions between integrins and the cytoskeleton: structure and regulation. In *Integrins: Molecular and Biological Responses to the Extracellular Matrix* (ed. D. A. Cheresh and R. P. Mecham), pp. 49-78. San Diego, CA: Academic Press.

Smilenov, L. B., Mikhailov, A., Pelham, R. J., Marcantonio, E. E. and Gunderson, G. G. (1999). Focal adhesion motility revealed in stationary fibroblasts. *Science* **286**, 1172-1174.

Tsuruta, D., Gonzales, M., Hopkinson, S. B., Otey, C., Khuon, S., Goldman, R. D. and Jones, J. C. R. (2002). Microfilament-dependent movement of the β3 integrin subunit within focal contacts of endothelial cells. *FASEB J.* **16**, 866-868.

Yoon, M., Moir, R. D., Prahlad, V. and Goldman, R. D. (1998). Motile properties of vimentin intermediate filament networks in living cells. *J. Cell Biol.* **143**, 147-157.

Zamir, E., Katz, M., Posen, Y., Erez, N., Yamada, K. M., Batz, B.-Z., Lin, S., Lin, D. C., Bershadsky, A., Kam, Z. et al. (2000). Dynamics and segregation of cell-matrix adhesions in cultured fibroblasts. *Nature Cell Biol.* **2**, 191-197.